

To be published the Astronomical Journal

The Formation and Evolution of Candidate Young Globular Clusters in NGC 3256

Stephen E. Zepf

Department of Astronomy, Yale University, New Haven, CT 06520;
zepf@astro.yale.edu

Keith M. Ashman

Department of Physics and Astronomy, University of Kansas, Lawrence, KS 66045;
ashman@kusphy.phsx.ukans.edu

Jayanne English

Space Telescope Science Institute, Baltimore, MD 21218; jenglish@stsci.edu

Kenneth C. Freeman

MSSSO, Private Bag, Weston Creek PO, 2611 Canberra, ACT, Australia;
kcf@merlin.anu.edu.au

Ray M. Sharples

Department of Physics, University of Durham, South Road, Durham, DH1 3LE, UK;
r.m.sharples@durham.ac.uk

ABSTRACT

We present images of the recent galaxy merger NGC 3256 obtained with the WFPC2 of the Hubble Space Telescope in *B* and *I* filters. We show that there is a large population of more than 1,000 compact, bright blue objects in this galaxy within the 7 kpc \times 7 kpc region studied. These objects have sizes, colors and luminosities like those expected for young Galactic globular clusters with ages ranging from a few to several hundred Myr. On this basis, we identify at least some fraction of the compact, bright blue objects in NGC 3256 as young globular clusters. The young cluster system comprises a significant fraction of the total luminosity of the galaxy within the region studied - 15 – 20% in *B* and half that in *I*, indicating a high efficiency of cluster formation on a galaxy-wide scale. In order to determine the properties of this young cluster system, the selection effects in size, color, and luminosity are carefully modeled. We find that the intrinsic color distribution is broad, and there is no significant trend of color with magnitude. The combination of the broad range of observed colors and the lack of a trend of redder colors at fainter magnitudes can not be fit solely by a broad age distribution and/or differential reddening, although the latter is clearly present.

The observations can be accounted for by either the preferential depletion/destruction of lower mass clusters as they age, or a very young age ($\lesssim 20$ Myr) for the cluster population, comparable to or less than the dynamical time of the region in which the clusters are observed. We also find that the luminosity function of the young cluster system can be roughly fit by a power-law with an exponent of -1.8, with tentative evidence that it flattens at faint magnitudes. The clusters are compact in size, with typical estimated half-light radii of five to ten parsecs, but there is no obvious cut-off for larger radii, and only a shallow trend of size with luminosity. We discuss the implications of these results for models of the formation and dynamical evolution of globular clusters, as well as for interpretation of the properties of older globular cluster systems.

Subject headings: galaxies: formation — galaxies: individual (NGC 3256) — galaxies: interactions — galaxies: starbursts — galaxies: star clusters

1. Introduction

Globular clusters have long been recognized as excellent fossil records of the formation history of their host galaxies (Ashman & Zepf 1998 and references therein). They also provide critical testbeds for the study of stellar evolution and stellar dynamics. However, the formation process of globular clusters themselves is not well understood. One hypothesis is that merger-induced starbursts are favorable environments for globular cluster formation (Schweizer 1987, Ashman & Zepf 1992). Ashman & Zepf (1992) specifically predicted that Hubble Space Telescope (HST) images of gas-rich mergers would reveal young globular clusters, readily identifiable through their very compact sizes, high luminosities, and blue colors. This prediction has been dramatically confirmed. Initial discoveries of compact, bright, blue star clusters in HST images of the peculiar galaxy NGC 1275 by Holtzman et al. (1992) and in the well-known galaxy merger NGC 7252 by Whitmore et al. (1993), have been followed up by the observations of similar objects with the characteristics of young globular clusters in a large number of starbursting and merging galaxies (see list in Ashman & Zepf 1998). The identification of these compact, bright, blue objects as young star clusters has been confirmed by ground-based spectroscopy in several systems (e.g. Schweizer & Seitzer 1998, Brodie et al. 1998, Zepf et al. 1995, Schweizer & Seitzer 1993). There are even possible mass estimates from high resolution spectroscopy of a few nearby examples (e.g. Ho & Filippenko 1997).

These observations provide significant support for the idea that globular clusters form in galaxy mergers and strong starbursts. They also suggest that globular cluster formation may be a regular part of the starbursting process. The empirical evidence for globular cluster formation in these environments is broadly consistent with the hypothesis that globular clusters primarily form in mergers and starbursts rather than in other sites. Other globular cluster formation scenarios

appear to have difficulties accounting for the observational properties of globular cluster systems (e.g. Ashman & Zepf 1998, Harris 1996 and references therein). In particular, correlations between cluster and host galaxy properties and the absence of dark matter are problematic for primordial globular cluster formation models (e.g. Peebles & Dicke 1968, Rosenblatt et al. 1988). Similarly, thermal instability models for globular cluster formation (e.g. Fall & Rees 1985) appear to be unable to account for the absence of a correlation between globular cluster metallicity and mass along with the high metallicities of typical globular clusters ($[\text{Fe}/\text{H}] > -1$).

The discovery of young globular cluster systems in nearby starbursts and galaxy mergers opens up the possibility of more detailed, empirical studies of the formation and evolution of globular clusters. One of the questions that remains to be answered is the efficiency with which globular clusters form in starbursts and mergers. This efficiency is critical for determining if most or all globular clusters can form in merger-like conditions. The efficiency can also constrain models of the formation the clusters themselves. For example, models in which globular clusters form as cores in much larger clouds predict low efficiencies, while models in which typical molecular clouds are compressed may be more efficient.

A closely related question is the dynamical evolution of globular cluster systems. Most studies to date have concentrated on developing theoretical models and matching these to the properties of old globular cluster systems that have undergone evolution over most of a Hubble time. Attempts to infer the initial population and the effects of evolution from the remnant population are difficult. Observations of young cluster systems can provide valuable input into the initial conditions and early dynamical evolution of globular cluster systems. This is not only true of the mass (luminosity) function, but also of the radii and densities with which the clusters form.

The efficiency of globular cluster formation in mergers and of the dynamical evolution of globular cluster populations also have significant implications for the use of globular cluster systems as fossil records of the formation history of their host galaxies. For example, Ashman & Zepf (1992) predicted that if elliptical galaxies form by mergers, they should have two or more populations of globular clusters. One of these populations originates from the halos of the progenitor spirals and is therefore spatially extended and metal-poor, while the other forms during the merger and is thus more spatially concentrated and metal-rich. This prediction of multiple populations in the globular cluster systems of ellipticals formed by mergers has now been confirmed in many cases (e.g. Ashman & Zepf 1998 and references therein). However, it has not yet been clearly demonstrated that the efficiency of cluster formation in galaxy mergers is sufficient to account for the metal-rich globular cluster population observed in elliptical galaxies. Furthermore, although there are strong theoretical arguments that the mass function of globular cluster systems evolves significantly over time to resemble the log-normal mass function of old globular cluster systems (e.g. Gnedin & Ostriker 1997, Murali & Weinberg 1997a), this evolution has not been demonstrated observationally.

The goal of this paper is to address the questions of the formation and evolution of globular

clusters through the study of the galaxy merger NGC 3256. The HST observations on which this study is based and the analysis of these data are presented in §2. The resulting sample of a large number of compact, bright, blue objects in NGC 3256 is examined in detail in §3. This section includes the determination of the relationship between the magnitudes, colors, and radii of the young cluster sample and the luminosity function. The implications of the results for the formation efficiency and dynamical evolution of globular cluster systems are discussed in §4, and the conclusions are given in §5.

2. Observations and Data Reduction

2.1. Target Galaxy

We utilized HST and WFCP2 to obtain high resolution images of the galaxy NGC 3256. This galaxy was selected for our program because it has long been identified as a galaxy merger (e.g. Toomre 1977) and is fairly nearby, with $cz_{\odot} = 2820 \text{ km s}^{-1}$ (English et al. 1999) which places NGC 3256 at a distance of 37 Mpc for $H_0 = 75 \text{ km s}^{-1} \text{ Mpc}^{-1}$. As shown in Figures 1 and 2 (plates 1 and 2), the central region of NGC 3256 has star forming knots, dust lanes, and loops, along with a more extended, smoother component. In the radio continuum and at 2.2μ there appear to be two nuclei separated by about 5'', or about 1 kpc (Norris & Forbes 1995, Kotilainen et al. 1996, Doyon, Joseph, & Wright 1994). Tidal tails can also be seen in the optical images in Figure 1, and have been shown to extend out to ~ 50 kpc in HI (English et al. 1999). Toomre (1977) placed it in the middle of his sequence of disk galaxy mergers, suggesting that it is dynamically older than the NGC 4038/4039 system (the Antennae), but younger than NGC 7252. Of the eleven mergers on the Toomre list, NGC 3256 also has the most molecular gas ($1.5 \times 10^{10} M_{\odot}$, Casoli et al. 1991, Aalto et al. 1991, Mirabel et al. 1990), and is the brightest in the far-infrared ($L_{FIR} = 3 \times 10^{11} L_{\odot}$, Sargent et al. 1989).

2.2. HST Observations

The WFPC2 images of NGC 3256 were obtained with the Planetary Camera (PC) centered on the galaxy. At a distance of 37 Mpc, each PC pixel is 8 pc, and the PC covers a total of 7 kpc \times 7 kpc, encompassing the starburst region identified in previous studies. The PC data centered on NGC 3256 are the subject of this paper. The data at larger radii will be discussed in future papers.

We imaged NGC 3256 in the F450W and F814W filters. Two equal exposures were obtained through each filter, with total exposures times of 1800s in F450W and 1600s in F814W. For each filter, the two exposures were combined utilizing a cosmic-ray rejection routine kindly provided by Rick White. As a check on this procedure, we also performed the more standard CCREJECT task

in STSDAS on the images in each filter, and then set a strict criterion for matching the object lists between the two filters. The final results were very similar to those produced by White's routine (c.f. Schweizer et al. 1996, Miller et al. 1997). A visual examination of the few differences favored the results of White's routine, so we used these combined images for further analysis. In any case, the number of compact sources observed is far greater than any possible residual defects. The resulting combined images are shown in Figure 2 (Plate 2).

2.3. Cluster Identification

A wealth of blue, compact objects is revealed in the HST images shown in Figure 2 (Plate 2). In order to determine the magnitudes and sizes of the compact objects discovered in the HST images, we first used the DAOFIND task in IRAF to identify objects. This task convolves the image with a Gaussian kernel, finds the best fitting Gaussian function at each point, and then searches for density enhancements which are both greater than a given threshold value and the brightest density enhancement in a localized region determined by the width of the Gaussian kernel. For this analysis, we set the FWHM of the Gaussian to be 2.8 pixels, which is the apparent width expected for an object with a true FWHM of roughly 2 pixels. We also applied broad cuts with the DAOFIND sharpness and roundness criteria to eliminate a few extremely diffuse or sharp features.

There are two notable effects of identifying objects in this standard way. One is that it introduces a selection bias against objects significantly larger than the smoothing kernel. This is a direct result of the search for density enhancements on a given scale. Although not an issue if all of the objects are unresolved or marginally resolved, this selection effect needs to be accounted for in studies of the distribution of object sizes. A second aspect of DAOFIND is that the threshold is defined globally. Several other globular cluster searches have been performed using a local threshold, rather than a global one (e.g. Kundu et al. 1998, Carlson et al. 1998, Miller et al. 1997). Although this has the advantage of giving a uniform number of false detections over the image, it does so at the cost of producing a non-uniform magnitude limit across the frame. As this is critical for our purposes, we retain the global threshold, and simply set it high enough that the probability of a spurious source in regions of high background (noise) is negligible. Perhaps the most critical aspect is that the detection algorithm is well-understood, and can be run on a variety of artificial datasets to explore the success with which it recovers objects of various luminosities, colors, and sizes.

2.4. Cluster Photometry

The next step is to determine the magnitudes of the identified objects. Because of crowding, variable background, and signal to noise, it is not possible to determine the brightness profile of the

objects out to large radius. Therefore we perform aperture photometry from one to several pixels in radius, and correct these modest apertures to total magnitudes. If the objects were unresolved, the aperture correction to total magnitude would be straightforward, as the HST point spread function (psf) is reasonably well-understood. Moreover, an aperture of several pixels incorporates the majority of the light from an unresolved source, even in the PC, so the overall correction is not a large one. However, the objects we detect in NGC 3256 are resolved, as expected for objects with sizes like those of Galactic globular clusters at the distance of NGC 3256. In this case, the aperture corrections depend on both the psf and the intrinsic radial profile of the object.

There is a limited amount of spatial information in the surface brightness profile within the few pixels radius out to which it can be reliably measured. Therefore, if a form of the profile is assumed, the radial scale of that profile can be determined by the difference between magnitudes at small radii. A Gaussian shape for the intrinsic profile of the clusters has been adopted in most previous work (e.g. Whitmore et al. 1993, Whitmore & Schweizer 1995, Schweizer et al. 1996). In order to facilitate comparison with these studies, we also adopt a Gaussian profile for the clusters, although we note that this will tend to underestimate the total magnitude if the clusters follow a more extended profile, such as a modified Hubble law (e.g. Holtzman et al. 1996, Carlson et al. 1998, Ostlin et al. 1998).

In detail, we determine the size of each object by comparing the difference between magnitudes within apertures of one and three pixels ($m_3 - m_1$) to a table of values for a wide range of Gaussian profiles convolved with the HST psf given by the TINYTIM software (Krist 1993). This is done in both the B and the I filters, and the resulting intrinsic FWHM is taken as the average of the two. We tested this procedure by using I-band (F814W) observations of unsaturated stars in the globular cluster Omega Cen as the basis for the HST psf. This psf gives the same inferred sizes as the TINYTIM psf when the intrinsic input FWHM is greater than about 0.5 of a PC pixel. For objects with intrinsic sizes less than 0.5 of a PC pixel, a slightly ($\sim 10\%$) smaller size is inferred with the Omega Cen psf than with the TINYTIM psf. This difference in inferred size due to different psfs is much smaller than the uncertainty introduced by the assumption of a form for the intrinsic surface brightness profile of globular clusters with only a single free parameter. Therefore, we adopt the TINYTIM results for the remaining analysis. We note that although the absolute errors in total magnitudes and half-light radii due to the requirement of an assumed profile form for the clusters in the sample can be significant, they should give good *relative* sizes and total magnitudes, providing the clusters are roughly similar to each other in structural characteristics. Moreover, any systematic error is likely to affect both filters, so that the colors will be mostly unaffected.

The total magnitude of each object is determined by applying the aperture correction from the magnitude within an aperture of 2 pixels in radius to a total magnitude, appropriate for the measured size for each object. This aperture correction for an object of typical size in our sample is roughly 0.85 magnitudes in B and 1.0 magnitudes in I. It compares to 0.25 magnitudes in B and 0.48 in I for completely unresolved objects. These differences emphasize both that our

objects are significantly resolved, and that the colors are largely unaffected by the correction to total magnitudes (cf. Holtzman et al. 1996). We correct the magnitudes and colors of the objects for Galactic reddening using the dust maps of Schlegel, Finkbeiner, & Davis (1998). These give $E(B - V) = 0.12$, and extinction in our HST filters of $A_{F450W} = 0.47$ and $A_{814W} = 0.23$. The absolute photometric calibration to the standard B and I_C system is achieved using the Holtzman et al. (1995) zero points for the F450W and F814W filters.

3. Analysis

The color, magnitude, and sizes of the objects detected in NGC 3256 are plotted in Figure 3¹. Several features of the cluster system of this galaxy merger are apparent in this diagram. One is the very large number of bright star clusters in this galaxy, approximately 1,000 with $M_B < -9$ inside of the central 7 kpc \times 7 kpc. These objects account for approximately 19% of the B light and 7% of the I light within this region. The star clusters generally have blue colors. The bright magnitudes and blue colors are indicative of massive star clusters at young ages. For reference, Figure 4 shows the prediction of two stellar population models for the color and magnitude of a $2 \times 10^5 M_\odot$ globular cluster as a function of age. The clusters are also compact like globular clusters, with typical sizes of $\lesssim 10$ pc. Only a few of the 1,000 objects are expected to be compact background galaxies or foreground stars, based on similar analyses of blank fields, such as the Hubble Deep Field.

In order to address the true distribution of the population in color, size, and magnitude, simulations of artificial datasets are required to calibrate the detection procedure. For example, the absence of objects with very faint B magnitudes and blue B-I colors may be caused by the detection limit in the I band. Similarly, the absence of large, faint clusters may also be possibly due to selection effects. Therefore, we created a grid of artificial objects with a range of magnitudes in each bandpass, and a range of sizes for each magnitude. By creating a full grid of artificial stars in both bandpasses, we can address the issue of any effect of incompleteness in B or I on the color distribution at faint magnitudes. The difference between input and output magnitudes also provides a calibration of the effect of “bin jumping” when constructing luminosity functions. Similarly, by incorporating a range of sizes in the artificial star tests, we can address the question of the intrinsic size distribution of the cluster population. This study is the first in which all of these effects have been modeled.

We can then test the consistency of various models of the luminosity, color, and sizes of the candidate globular clusters in NGC 3256 against the observations. Specifically, we create model data sets with various combinations of luminosity functions, color-magnitude relations, and

¹The positions, magnitudes, colors, and sizes of the objects found in NGC 3256 are also given in Table 1, available either in the electronic journal or from the first author.

luminosity-size relations. For the luminosity function and luminosity size-relation, we adopt a power-law form, while we use a linear relation between color and magnitude. The intrinsic widths of the color and size distributions are drawn from the data at bright magnitudes where they are unaffected by selection. Predictions for observables for each model are made by convolving the model with the selection functions derived from the simulations described above.

We compare these predictions of various models to the luminosity function, color-magnitude relation, and luminosity-size relation observed for the candidate young globular clusters in NGC 3256 (Figure 3). A model is considered to fit the color-magnitude and luminosity-size relation if the linear regression of these parameters is statistically consistent with the data. To insure that the results are not dependent on the use of a linear fit, we also compare the median colors and sizes as a function of magnitude of the models to the observations, with the uncertainties in the medians of the data determined via bootstrapping. For the luminosity function, the goodness of the fit is determined using the double-root-residual test (Ashman, Bird, & Zepf 1994). We also test the effects of changes in any one of the underlying distributions on all of the observed properties, as they are not decoupled from each other. For example, an underlying luminosity function can be flat, but if the clusters are smaller at faint magnitudes, they will be easier to detect, and the luminosity function will appear to rise at faint magnitudes. Similarly, a trend of color with magnitude can also give rise to an apparent luminosity function different than the underlying one if different color clusters are detected with different efficiency at faint magnitudes.

We find that the best fitting model cluster population has little or no correlation between luminosity and color (B-I independent of M_B), a shallow correlation between luminosity and radius ($r \propto L^{0.07}$), a power-law luminosity function $N(L) \propto L^{-1.8}$. This best fitting model is shown in Figure 5. The statistical uncertainties on the parameters of the underlying cluster population are roughly 0.05 in the slope of the magnitude-color relation, and 0.1 in the exponent of both the radius-luminosity relation and the luminosity function. We discuss the magnitude-color relation, luminosity-size relation, and luminosity function individually in more detail below.

3.1. Color-Magnitude Relation

The broad color distribution and absence of a strong relationship between color and luminosity places strong constraints on the nature and evolution of the young cluster system in NGC 3256. In order to produce the observed range of colors, either differential reddening by dust or a range of ages is required. However, both reddening and age generally produce fainter magnitudes for redder objects (see Figure 4). This is not observed in NGC 3256, as shown by the similar color-magnitude diagrams of the data (Figure 3) and a simulated data set with no relationship between color and magnitude (Figure 5). A quantitative measure of the close agreement between the observations and a simulated data set with no relationship between color and magnitude is the similar median (B-I) colors as a function of B magnitude, which are given in Table 2. In contrast, a simulated

data set with an intrinsic slope of $(B-I) \propto 0.5B$, like that expected for a standard reddening law, gives a much steeper relation between $(B-I)$ color and B magnitude, as shown in Table 2. Similar results are obtained using other robust measures of the average color as a function of magnitude. The fundamental result is that we are unable to account for the broad range of observed colors solely by differential reddening or a broad age distribution because there is no intrinsic trend of redder colors with fainter magnitudes.

The observations can be accounted for in two ways. One possibility is that the young cluster system in NGC 3256 has an age distribution up to several hundred Myr *and* low mass clusters are preferentially destroyed over this timescale. In this way, the typical luminosity of the older, redder cluster population will not become much fainter than the younger bluer, cluster population because the younger population will have more low-mass clusters. A modest amount of reddening may also be required to produce the colors of the reddest clusters, but not so much that a strong color-luminosity trend is produced.

The lack of a strong color-luminosity relation can also be accounted for if most of the clusters are very young. At ages up to ~ 10 Myr, stellar population models predict a fairly broad range of colors with little change in B luminosity (see Figure 4). This effect is due to red supergiants, and is stronger in the Leitherer et al. (1998) models than the Bruzual & Charlot (1998) models because of the increased presence of red supergiants in the former models. As in the previous case, some reddening may be required to produce the reddest clusters, but reddening can not be the primary determinant of the cluster colors, or a color-magnitude relation would be introduced, contrary to the observations. The critical aspect of the possibility that red supergiants at young ages account for much of the observed color spread is the requirement of a very young age for the system as a whole because all of the models begin to produce a significant color-luminosity trend after ~ 10 Myrs.

Both the destruction and red supergiant hypotheses can account for a broad color distribution without a strong color-luminosity relation. An additional constraint is that the range of ages in the young cluster population would not be expected to be less than the dynamical time of the region in which they formed. Adopting a radius of 3 kpc for the region in which the young clusters are found, and a typical velocity of $v \approx 150$ km s $^{-1}$, we find a dynamical time of 20 Myr. Thus the very young age hypothesis is marginally inconsistent with the requirement that the cluster population not form on a timescale shorter than the dynamical time. Other explanations for the absence of a strong color-luminosity trend are strongly constrained by the large observed color spread. For example, a model in which younger clusters are more heavily reddened than older clusters can give a weak color-luminosity trend. However, it does so at the cost of narrowing the color spread, and therefore fails to account for the observations.

3.2. Luminosity-Radius Relation

A second observation of relevance for models of the formation and evolution of young star clusters is the luminosity-radius relationship. The NGC 3256 young star cluster system has a very shallow relationship between radius and luminosity, roughly $r \propto L^{0.07}$. The relationship of radius with mass is likely to be similar to that with luminosity. This follows from the absence of a correlation between color and luminosity which suggests the mass-to-light ratio is mostly independent of luminosity. Thus, cluster mass is likely to be fairly independent of radius.

A weak correlation between mass and radius has significant implications for the formation and evolution of globular clusters. Clouds in hydrostatic equilibrium follow the relationship $r \propto M^{1/2}P^{-1/4}$ (e.g. Ashman & Zepf 1999, Elmegreen 1989). The shallow observed correlation between radius and mass therefore suggests that higher mass clusters form at higher pressure. If confirmed, this will play a significant role in developing models of globular cluster formation.

A shallow relationship between mass and radius also suggests that on average low-mass clusters are formed with lower density and are less bound than higher mass clusters. Therefore, they will be more susceptible to destruction by mass loss at early ages, and through tidal shocks over time. This result is an important input into determinations of the effect of dynamical evolution on the mass function of clusters, as discussed in the previous and the following subsections. In particular, studies of the dynamical evolution of globular cluster systems must adopt some relation between radius and mass for the initial cluster population (e.g. Ostriker & Gnedin 1997 and references therein). Without data from young clusters, this relation has been based on observations of old cluster populations, whose properties may have already been altered by dynamical evolution. Thus, observations of the radii of young cluster systems are an important part of the study of dynamical evolution of globular cluster systems.

These conclusions regarding the mass-radius relationship require confirmation, as the clusters are only marginally resolved in the present data. We are able to recover differences in the sizes of the objects, given a form for the radial profile of the cluster. The inferred mass-radius relationship for the cluster population should not be sensitive to the form of the profile adopted because it is only based on relative values of cluster radii. Therefore, our result is not likely to be sensitive to the specific cluster profile chosen, although it will be affected by any systematic changes in the shape of the profile with cluster mass.

3.3. Luminosity Function

The luminosity function of the NGC 3256 cluster system has a best-fitting power with slope about -1.8 , with tentative evidence that it flattens at faint magnitudes. This slope is similar to that found in other young globular cluster systems in galaxy mergers (e.g. Whitmore & Schweizer 1995, Schweizer et al. 1996, Miller et al. 1997, Carlson et al. 1997) and also to that for populous

clusters in the LMC (Elmegreen & Efremov 1997, Elson & Fall 1985). The most notable difference between the observed luminosity function and a power-law convolved with observational selection is that the data appear to be flatter at the faint end than the model. In order to assess the statistical significance of this difference, we utilized a double-root-residual test (Ashman et al. 1994). The test indicates the difference is significant at about the 2.5σ level. However, given the uncertainties modeling the selection at these faint levels, any deviation from a power-law slope is tentative. Although the luminosity function of the NGC 3256 cluster system is now roughly a power-law, both the luminosity-color and luminosity-radius relation suggest that it is likely to evolve significantly over time. This is also expected on theoretical grounds (e.g. Gnedin & Ostriker 1997, Murali & Weinberg 1997a). A comparison of the observations to these theoretical expectations is presented below.

4. Discussion

HST imaging of the galaxy merger NGC 3256 has revealed a large population of objects with the bright luminosities, blue colors, and compact sizes expected of objects like Galactic globular clusters at young ages. In this section, we explore in more detail the relation of young clusters observed in starbursting and merging galaxies like NGC 3256 to old globular clusters, and to implications these observations have for models of the formation of globular clusters.

4.1. Cluster Mass Function and Dynamical Evolution

The power-law luminosity function is the one feature of the NGC 3256 young cluster system that is decidedly different from that of old globular cluster systems around galaxies like M87 and the Milky Way, which have lognormal luminosity functions. Although the masses and sizes inferred for many of the young clusters in NGC 3256 are similar to those of old globular clusters (e.g. Figures 3 and 5), the difference in the shape of the luminosity function has long been used to argue that the clusters in mergers and starbursts are fundamentally different than in the old systems (e.g. van den Bergh 1995). However, it has also long been realized that dynamical evolution can significantly alter the mass function of clusters systems over a Hubble time (e.g. Fall & Rees 1977, Gnedin & Ostriker 1997, Murali & Weinberg 1997a, 1997b, Ashman & Zepf 1998 and many references therein).

We therefore consider whether observations of the mass and luminosity functions of cluster systems over a range of ages can be consistently accounted for by dynamical evolution. The two long-term dynamical processes that may be relevant for determining the shape of the globular cluster mass function are evaporation and tidal shocking. These have the following scalings between the lifetime of a cluster and its mass and radius $t_{evap} \propto M^{1/2} r^{3/2}$, and $t_{sh} \propto M r^{-3}$. The timescale for tidal shocks also depends on the cluster orbit and galaxy potential. As long as

these are similar in the galaxies being compared, the scaling is independent of these parameters. Therefore, we concentrate on the scaling of the destruction timescale with cluster mass and radius.

In §3.2, we found that cluster mass and radius may be only weakly dependent on one another with $r \propto L^{0.07}$. With this result, the equations above give a timescale for destruction that scales as roughly $M^{2/3}$ for both evaporation and tidal shocking. These give relative timescales for destruction of clusters as a function of their mass. An absolute timescale can be placed on these scalings through the known turnover mass and age of the globular cluster systems of galaxies like the Milky Way and M87. This allows us to determine the cluster mass scale that is undergoing destruction at the ages corresponding to young cluster systems observed in galaxy mergers. In this way, we find that at an age of 100 Myr, the characteristic mass scale set by dynamical processes is 10^{-3} of that for the globular cluster systems of the Milky Way and M87. At 500 Myr the corresponding number is about 10^{-2} of the characteristic mass scale of old globular cluster systems. This calculation is also based on the simplifying assumption that the dynamical processes are independent of one another, which is not strictly true. However, the numbers given above are not likely to be dramatically wrong as long as the observation that M and r are mostly independent holds.

If long-term dynamical processes are responsible for evolution of the mass function, the above calculation suggests the “turnover” in the mass function in young globular cluster systems will occur at much smaller masses than in older globular cluster systems like that in the Galaxy. These small masses make such a turnover very difficult to observe directly in young systems. Specifically, the above calculation suggests that clusters with masses of roughly 1% of the current turnover mass are being destroyed at the ages typical of young globular cluster systems, such as the NGC 3256 system studied here, as well as the NGC 1275 system (Carlson et al. 1998) and the NGC 7252 system (Miller et al. 1997). This corresponds to clusters five magnitudes below the current turnover of the globular cluster luminosity function.

In order to calculate the detectability of a dynamically induced turnover in young cluster systems, the expected brightening of young clusters must also be accounted for. Stellar populations models (e.g. Bruzual & Charlot 1998) predict that old objects of this magnitude were about 5.0 magnitudes brighter in B and 3.7 in V at the ages inferred for NGC 3256 from their colors. The corresponding brightening for the slightly older NGC 1275 and NGC 7252 cluster systems we will also study is about 4.2 magnitudes in B and 3.1 in V. The predicted brightening in these young cluster systems relative to ~ 13 Gyr old populations is dependent primarily on the mass function between several M_\odot and slightly less than one M_\odot . The adopted numbers are for a Salpeter (1955) slope of $x = 1.35$ are somewhat less for flatter mass functions.

The net result is that in young cluster systems observed in the B-band, such as NGC 3256, the observations must reach absolute magnitudes around the current turnover luminosity in old globular cluster systems, roughly $B = -6.8$. As can be seen in Figure 3, the observations fail by several magnitudes to reach such faint levels. In fact, it will be difficult to obtain reliable

cluster counts at such magnitudes because of potential confusion with individual bright stars, which can have similar luminosities. Analyses of the NGC 1275 and NGC 7252 datasets give similar conclusions that the highest mass scale at which dynamical evolution is expected to be effective is well below the observational limit. In particular, for these ~ 500 Myr old systems, the observations would have to reach limits of about $B \gtrsim -6$ and $V \gtrsim -5.5$, while the observations are limited to about two magnitudes brighter.

The luminosity functions of known cluster systems are therefore consistent with a model in which globular clusters form with a power-law mass function, and evolve through well-known dynamical processes to have the log-normal mass function observed in old systems such as the Milky Way and M87. Testing this hypothesis by directly looking for the turnover in young cluster systems is difficult because the mass scale is predicted to be extremely small. This work suggests that searches for turnovers in globular cluster mass functions might be more profitable in more intermediate-age systems in which the predicted mass scale may be accessible to observation.

In order to improve the predictions for the dynamical evolution of young globular cluster systems, better constraints on the initial mass-radius relation are required. Studies of young cluster systems are critical for providing these constraints because these systems have not undergone as much dynamical evolution and will more accurately reflect the relationship between mass and radius at the time the young clusters formed. This relation plays a major role in the dynamical calculations. Specifically, the timescales for evaporation and tidal shocking depend on both mass and radius. If the relationship between mass and radius is stronger than it appears to be in our observations of the NGC 3256 system, the timescales for disruption of clusters of different masses will be affected. For example, if $r \propto M^{1/2}$, then t_{evap} will have a very steep dependence on mass, and t_{sh} will be shorter for larger masses. In this case, the mass scale for evaporation at 100 Myr would be only about a factor of 5 less than that after 10 Gyr, and only a factor of 3 less at 500 Myr compared to 10 Gyr. However, the tidal shocking would then be inversely correlated with mass, so both high and low mass clusters would be destroyed and the observational predictions in this case are less clear.

Perhaps the safest conclusion then from our analysis of the formation and destruction of globular clusters is that information on the radii of the clusters as well as their mass function is critical for determining the effects of dynamical evolution and comparing of mass functions of young and old cluster systems. The cluster radii and mass-radius relation also have significant implications for models of the formation of young globular clusters. Further exploration of observational constraints on the initial mass-radius relation is a promising route for future studies.

4.2. Efficiency of Compact, Massive Cluster Formation

The census of compact, young star clusters in NGC 3256 allows the determination of the efficiency with which clusters form. The simplest characterization of efficiency is the fraction of

new stars formed that are in dense star clusters. As described in §3.1, this fraction is about 20% based on the percentage of blue light that is in dense star clusters. This value is similar to that observed in smaller starburst regions by Meurer et al. (1995). It is somewhat larger than the fraction of blue light in dense star clusters observed in the older NGC 7252 system, suggesting that either the formation efficiency peaks near the peak of the starburst or the dynamical evolution removes some of the clusters on the timescale of the age of the NGC 7252 system. A critical aspect of these NGC 3256 data is that they demonstrate that high formation efficiency can occur over a large area ($7 \text{ kpc} \times 7 \text{ kpc}$) encompassing much of a $\sim L_*$ galaxy. These data also indicate that the fraction of stars that form in these dense star clusters is not negligible, and suggest that this is an interesting mode of star formation.

A second way to characterize the efficiency of cluster formation is to compare it to the total amount of gas available. This is less straightforward than comparing the fraction of light, but connects more directly to current theoretical models. The total amount of molecular gas inferred from CO observations and standard assumptions regarding the conversion to H₂ mass is $1.5 \times 10^{10} M_\odot$ (Casoli et al. 1991, Aalto et al. 1991, Mirabel et al. 1990). The total mass in the young cluster system can be estimated from the color of each object, and a stellar populations model that allows color to be converted to age and mass-to-light ratio. The observed luminosity can then be converted into mass. Applying this procedure individually to each cluster in the NGC 3256 cluster sample and summing up gives a total mass in the young cluster system of $6 \times 10^7 M_\odot$. This is based on taking all objects with $(B - I) < 1.5$ and inferred sizes less than 15 pc, and using the Charlot-Bruzual stellar population models with a Miller-Scalo initial mass function. A Salpeter initial mass function would increase the mass estimate by approximately 50%. Reddening of observed objects is less of a factor because its effects on the mass estimate cancel out to first order. Specifically, reddening makes the objects fainter, decreasing the apparent luminosity, but also redder, increasing the inferred mass-to-light ratio, so in the end the mass estimate is similar. For example, the mass estimate for the NGC 3256 cluster system is only about 30% greater for an internal reddening of $A_B = 1.0$ compared to $A_B = 0.0$. An additional effect is that some clusters may be extincted beyond detection.

The resulting efficiency for the formation of massive, compact clusters computed in this way is then about 0.5%. This is a lower limit in the sense that cluster formation is ongoing and there is plenty of gas mass left from which to form more clusters. If clusters continue to make up $\sim 20\%$ of the stars formed, the total cluster mass fraction at the end of the starburst will be closer to this value. Therefore, the observations place the formation efficiency between 0.5 – 20% depending on how exactly efficiency is defined and what happens in the future of the starburst in NGC 3256.

It is interesting to compare our observed efficiency of globular cluster formation in NGC 3256 to the fraction of mass in old stellar populations that is in globular clusters. The highest observed fraction of mass in globular clusters to total stellar mass is about 1%, as seen in the Galactic halo and the richest extragalactic globular cluster systems such as M87 (e.g. Ashman & Zepf 1998). Typical elliptical galaxies have ratios about five times lower, around 0.2%. Therefore, the

globular cluster formation efficiency observed in NGC 3256 is more than sufficient to account for the globular cluster systems of elliptical galaxies. More specifically, if the mass fraction of stars that form in globular clusters is closer to 20% over the full starburst/merger event, then mergers have an over-efficiency problem.

This over-efficiency problem can be alleviated in several ways. One possibility is that the progenitor spirals are gas-poor, which may be true at the current epoch but seems unlikely at high redshift when most mergers are likely to occur. A more likely explanation is significant dynamical destruction of the cluster population. This destruction is predicted by theory and required by observation if the power-law luminosity functions of young cluster systems are to match the lognormal luminosity function of old globular cluster systems. Conversely, if the overall mass fraction of stars that form in globular clusters is closer to 0.5%, then gas-rich mergers will make about the right number of globular clusters for moderately rich systems, and gas-poor mergers will lead to moderately poor globular cluster systems. The reality is likely to be somewhere between these two extremes. It is unlikely that all globular cluster formation in NGC 3256 will immediately cease while the large reservoir of cold gas continues to form stars, as required for the overall efficiency to be 0.5%. It is also unlikely that all of the remaining gas will form stars in a starburst in which 20% of the new stars are formed in dense, massive clusters, as is currently happening in NGC 3256. Moreover, many clusters are expected to be lost due to dynamical processes.

The high efficiency of globular cluster formation observed in NGC 3256 also has significant implications for theoretical models of globular cluster formation. In particular, scenarios in which globular clusters form as cores within proposed super giant molecular clouds (SGMCs) predict that only about $\sim 0.2\%$ of the mass of the cloud forms stars in dense cores, as seen in Galactic giant molecular clouds (McLaughlin & Pudritz 1996, Harris & Pudritz 1994). Thus the observed globular cluster formation efficiency appears to pose a problem for the SGMC scenario. A second problem is the long timescale for the formation of SGMCs in these models compared to the apparently rapid formation of globular clusters in galaxy mergers and starbursts. The observations appear to be more consistent with models of globular cluster formation in which the clusters form from highly compressed giant molecular clouds of typical mass for spiral galaxies. These may either originate from the progenitor spirals or be newly made GMCs.

4.3. Conclusions

The primary conclusions of our study of HST images in B and I of the galaxy merger NGC 3256 are:

1. NGC 3256 has a very large population of compact, bright, blue objects. Many of these clusters have estimated sizes and masses like those of Galactic globular clusters. On this basis, we identify some fraction of these objects as young globular clusters.
2. The young cluster system has a broad range of colors, but little or no correlation between color

and luminosity. This observation requires either destruction of low mass clusters over time or a very young age ($\lesssim 20$ Myr) for the young cluster system.

3. Dynamical evolution is likely to significantly affect the mass function of the young cluster system. If the system is not very young, this has already been observed. The mass-radius relation for the cluster population is an important constraint on the predictions for dynamical evolution of the cluster population.
4. The large number of candidate young globular clusters indicates a high efficiency of cluster formation. This is observed across the 7 kpc \times 7 kpc region studied. The efficiency of cluster formation in the galaxy merger NGC 3256 is more than sufficient to account for the metal-rich globular cluster populations in elliptical galaxies if these form from gas-rich mergers.

We thank Richard Larson for useful discussions, Dave Carter for collaborating in obtaining the AAT image of NGC 3256, and Eddie Bergeron for making the color images from the HST data. We thank an anonymous referee for helpful suggestions. S.E.Z. and K.M.A. acknowledge support for this project from NASA through grants GO-05396-94A and AR-07542-96A awarded by the Space Telescope Science Institute, which is operated by the Association of Universities for Research in Astronomy, Inc., for NASA under contract NAS 5-26555. SEZ also acknowledges the support of a Hubble Fellowship and fruitful discussions with colleagues at UC Berkeley during the early stages of this work.

REFERENCES

Aalto, S., Black, J.H., Booth, R.S., & Johansson, L.E.B 1991, *A&A*, 247, 291
Ashman, K.M., & Zepf, S.E. 1992, *ApJ*, 384, 50
Ashman, K.M., Bird, C.M. & Zepf, S.E. 1994, *AJ*, 108, 2348
Ashman, K.M., & Zepf, S.E. 1998, *Globular Cluster Systems* (Cambridge University Press: Cambridge).
Ashman, K.M., & Zepf, S.E. 1999, *ApJ*, in preparation
Brodie, J. P., Schroder, L. L., Huchra, J. P., Phillips, A. C., Kissler-Patig, M., & Forbes, D. A. 1998, *AJ*, 116, 691
Bruzual, A.G., & Charlot, S. 1998, *ApJ*, in preparation
Carlson, M.N. et al. 1998, *AJ*, 115, 1778
Casoli, F., Dupraz, C., Combes, F., & Kazes, I. 1991, *A&A*, 251, 1
Doyon, R., Joseph, R.D., & Wright, G.S. 1994, *ApJ*, 421, 101
Elmegreen, B.G. 1989, *ApJ*, 338, 178

Elmegreen, B.G., & Efremov, Y.N. 1997, *ApJ*, 480, 235

Elson, R.A.W., & Fall, S.M. 1985, *PASP*, 97, 692

English, J., Norris, R. P., Freeman, K. C., & Booth, R. S. 1998, in preparation

Fall, S.M., & Rees, M.J. 1977, *MNRAS*, 181, 37

Fall, S.M., & Rees, M.J. 1985, *ApJ*, 298, 18

Gnedin, O.Y., & Ostriker, J.P. 1997, *ApJ*, 474, 223

Harris, W.E. 1996, in *Formation of the Galactic Halo...Inside and Out*, eds. H. Morrison & A. Sarajedini, (San Francisco: ASP), 231

Harris, W.E., & Pudritz, R.E. 1994, *ApJ*, 429, 177

Ho, L.C., & Filippenko, A.V. 1996, *ApJ*, 466, L83

Holtzman, J.A., et al. 1992, *AJ*, 103, 691

Holtzman, J.A., et al. 1996, *AJ*, 112, 416

Isobe, T., Feigelson, E.D., Akritas, M.G., & Babu, G.J. 1990, *ApJ*, 364, 104

Kotilainen, J. K.; Moorwood, A. F. M.; Ward, M. J.; Forbes, D. A. 1996, *A&A*, 305, 107

Krist, J. 1993, in *Astronomical Data Analysis Software and Systems II*, eds. R.J. Hanisch, R.J.V. Brissenden, & J. Barnes, *ASP Conference Series* 52, 536

Leitherer, C. et al. 1999, *ApJS*, submitted

McLaughlin, D.E. & Pudritz, R. 1996, *ApJ*, 457, 578

Meurer, G. R., Heckman, T. M., Leitherer, C., Kinney, A.; Robert, C., & Garnett, D. R. 1995, *AJ*, 110, 2665

Miller, B.W., Whitmore, B.C., Schweizer, F., & Fall, S.M. 1997, *AJ*, 114, 2381

Mirabel, I.F., Booth, R.S., Johansson, L. E. B., Garay, G., & Sanders, D.B. 1990, *A&A*, 236, 327

Murali, C., & Weinberg, M.D. 1997a, *MNRAS*, 288, 749

Murali, C., & Weinberg, M.D. 1997b, *MNRAS*, 288, 767

Norris, R.P., & Forbes, D.A. 1995, *ApJ*, 446, 594

Ostlin, G., Bergvall, N., & Ronnback, J. 1998, *A&A*, 335, 850

Ostriker, J.P., & Gnedin, O.Y. 1997, *ApJ*, 487, 667

Peebles, P.J.E., & Dicke, R.H. 1968, *ApJ*, 154, 891

Rosenblatt, E.I., Faber, S.M., & Blumenthal, G.R. 1988, *ApJ*, 330, 191

Salpeter, E. E. 1955, *ApJ*, 121, 161

Sargent, A.I., Sanders, D.B., & Phillips, T.G. 1989, *ApJ*, 346, L9

Schlegel, D.J., Finkbeiner, D.P., & Davis, M. 1998, *ApJ*, 500, 525

Schweizer, F., & Seitzer, P. 1993, *ApJ*, 417, L29

Schweizer, F., Miller, B.Y., Whitmore, B.C., & Fall, S.M.F. 1996, *AJ*, 112, 1839

Schweizer, F., & Seitzer, P. 1998, *AJ*, 116, 2206

Toomre, A. 1977, in *The Evolution of Galaxies and Stellar Populations*, eds. B. Tinsley & R. Larson (Yale Univ. Press), 401

van den Bergh, S. 1995, *Nature*, 374, 215

Whitmore, B.C., Schweizer, F., Leitherer, C., Borne, K., & Robert, C. 1993, *AJ*, 106, 1354

Whitmore, B.C., & Schweizer, F. 1995, *AJ*, 109, 960

Whitmore, B.C., & Schweizer, F. 1997, *AJ*, 114, 1797

Zepf, S.E., & Ashman, K.M. 1993 *MNRAS*, 264, 611

Zepf, S.E., Carter, D., Sharples, R.M., & Ashman, K.M. 1995, *ApJ*, 445, L19

Table 2. Median Color of Objects as a Function B Magnitude

m_B	Observed (B-I) _{med}	90% confidence limits ^a	Model:(B-I) \neq B	Model:(B-I) \propto 0.5B
19.25	0.85	0.81-1.10	0.67	0.36
19.75	0.69	0.66-0.80	0.64	0.38
20.25	0.67	0.60-0.75	0.64	0.42
20.75	0.71	0.64-0.81	0.67	0.54
21.25	0.66	0.57-0.69	0.67	0.65
21.75	0.76	0.70-0.83	0.68	0.85
22.25	0.82	0.77-0.87	0.73	1.10
22.75	0.78	0.75-0.84	0.79	1.22
23.25	0.91	0.87-0.94	0.90	1.36
23.75	1.03	1.00-1.10	1.06	1.44

^aConfidence limits determined via bootstrap

Fig. 1.— An R-band image of NGC 3256 obtained with the AAT. The image is 6.6' on a side and is the average of a total of 80 minutes of integration.

Fig. 2.— HST color images of NGC 3256. The first figure is for the two WFPC2 pointings combined, while the second is a blow-up of the central PC which is the subject of this study. The color is created by using the image in the B-band for the blue input, a combined B+I image for the green, and the I-band image for the red.

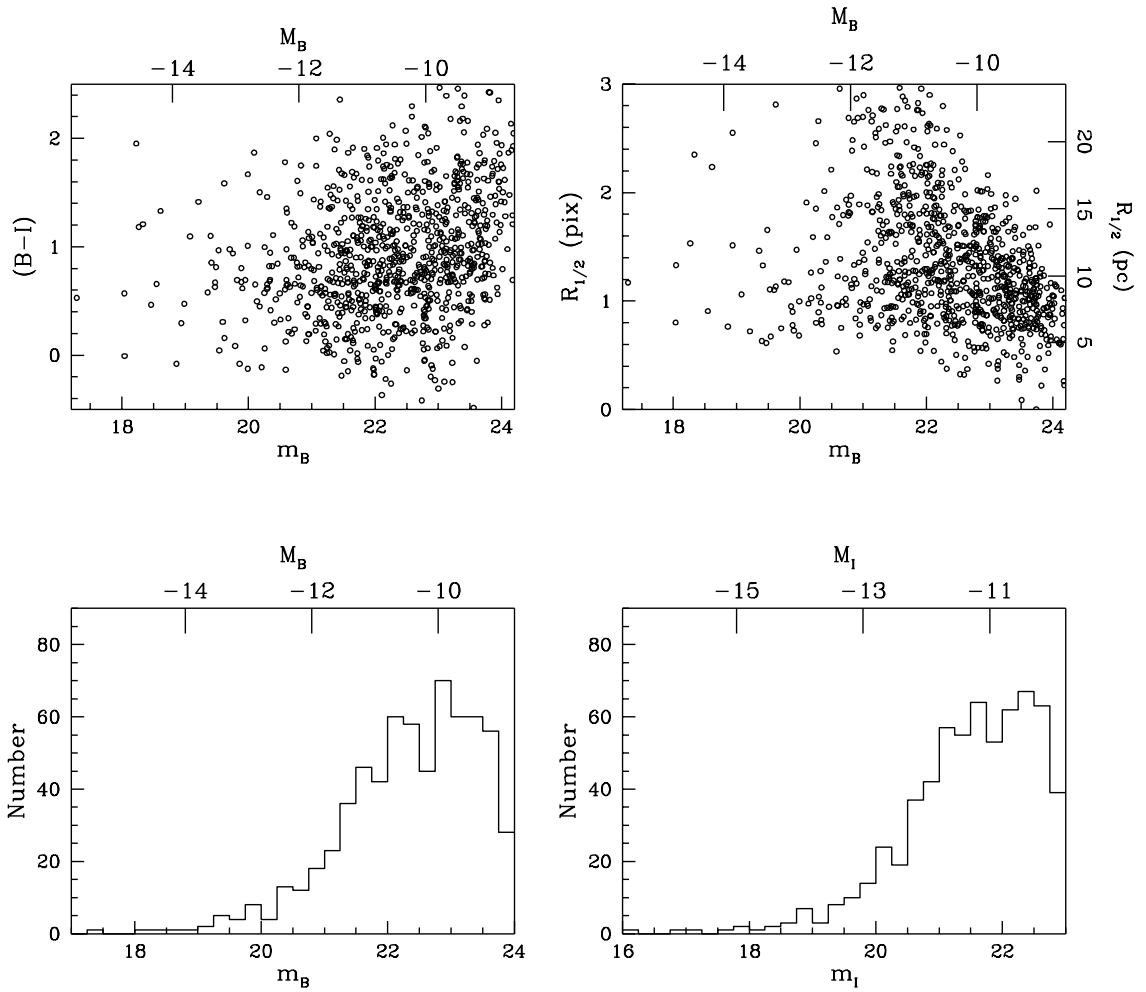


Fig. 3.— Observed properties of the population of young globular clusters in NGC 3256. In the upper left panel, the colors of the clusters are plotted against their magnitudes. The upper right panel shows the estimated cluster radii plotted against their magnitudes. The luminosity function of the young cluster system is plotted in the lower panel.

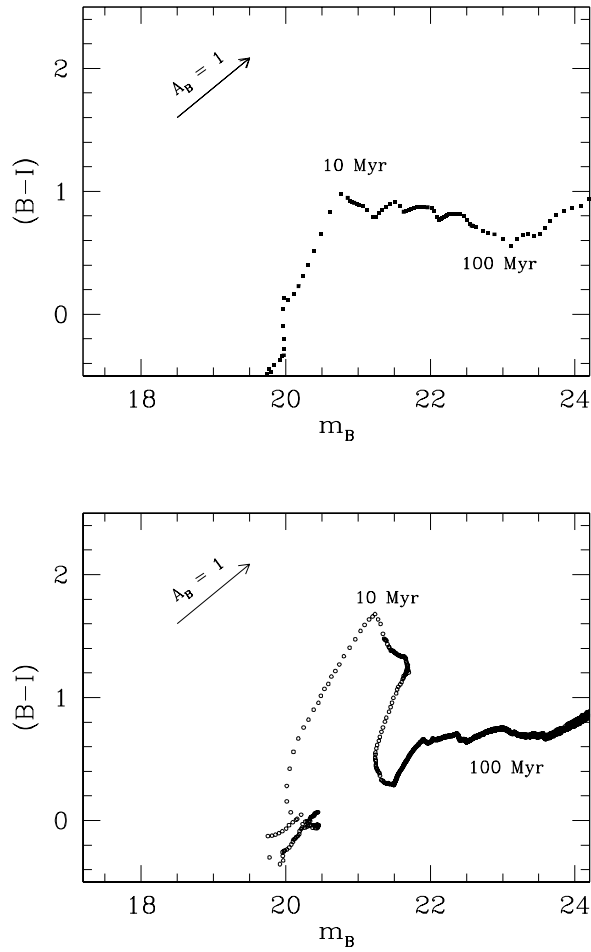


Fig. 4.— Plots of the time evolution in color and magnitude of a $2 \times 10^5 M_{\odot}$ star cluster. The upper panel is based on the Bruzual & Charlot (1998) stellar populations models and the lower panel on the Leitherer et al. (1999) models. The effect of extinction of one magnitude in B and a Galactic extinction law is noted by the arrow in each plot, and the apparent magnitude determined for a distance to NGC 3256 of 37 Mpc.

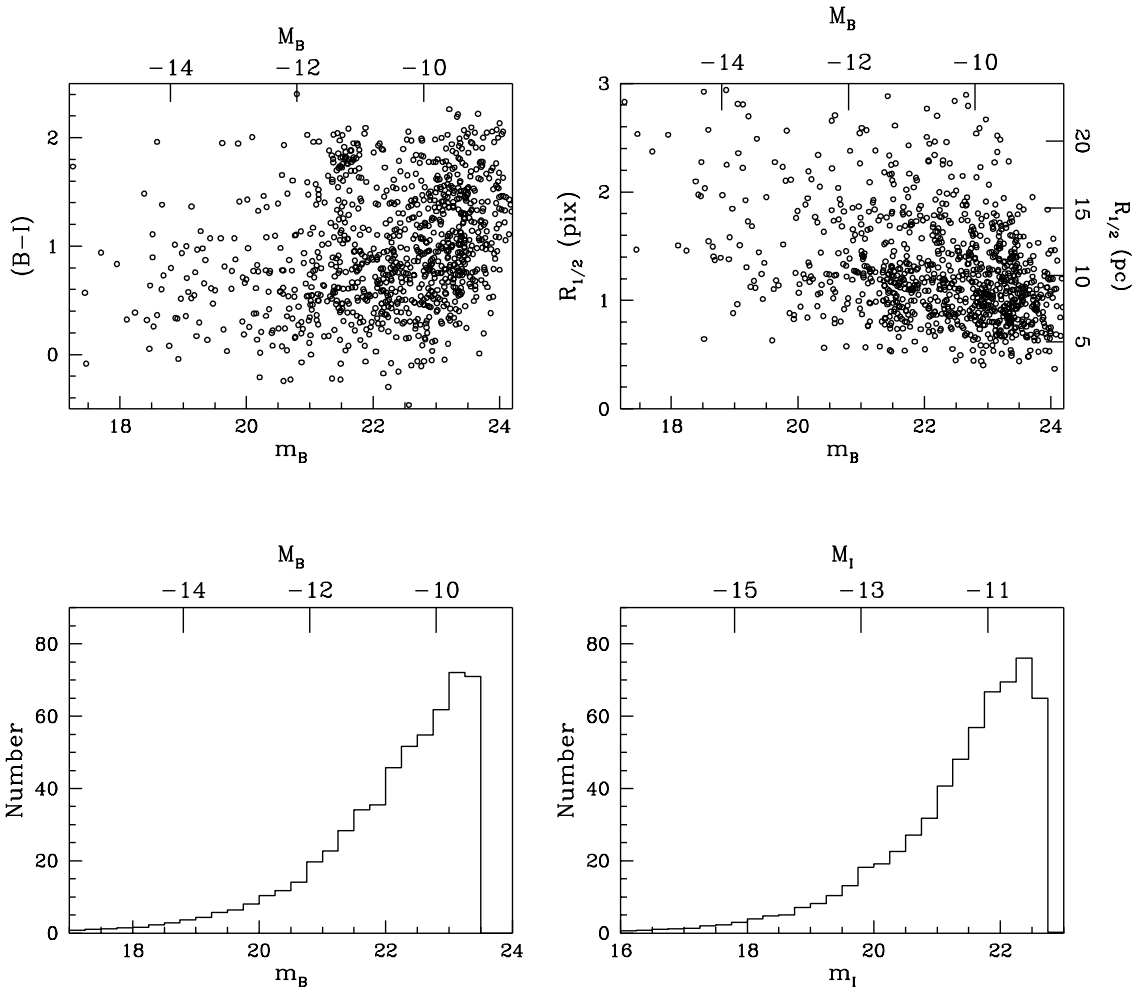


Fig. 5.— The properties of the simulated data set which best matches Plots of the NGC 3256 candidate young globular cluster sample compared to a simulated dataset which is the convolution of selection effects with an input model with $N \propto L^{-1.8}$, $R_{1/2} \propto L^{0.07}$, and no correlation between $(B - I)$ and B .